land

MDPI

Article

Zoning Management Based on Spatiotemporal Evolution of Ecological Risk: Spatial Network Analysis of Riparian Zone in Lanzhou–Baiyin Metropolitan Area of the Yellow River Basin

Zhijie Chen [1,2,*], Jiayue Yang [1], Miao Han [1], Haoxin Wang [1] and Yongrui Song [1]

[1] School of Architecture and Urban Planning, Lanzhou Jiaotong University, Lanzhou 730070, China; 12241884@stu.lzjtu.edu.cn (J.Y.); 12251974@stu.lzjtu.edu.cn (M.H.); 11250609@stu.lzjtu.edu.cn (H.W.); 12231841@stu.lzjtu.edu.cn (Y.S.)
[2] School of Architecture, Tianjin University, Tianjin 300072, China
* Correspondence: zhjchen@lzjtu.edu.cn

Abstract

The upper Yellow River basin is a classic ecologically vulnerable area, characterized by acute human–land conflicts. The rapid pace of urbanization drives landscape fragmentation, which severely threatens regional sustainability and ecological security. Given the difficulty of using a single indicator to fully diagnose the relationship between ecological function and risk, this research establishes a spatial diagnostic framework that uses ecosystem service value (ESV) to measure functional output and landscape ecological risk (LER) to indicate structural vulnerability. Utilizing land use data from 1990 to 2020, we quantified, for the first time at a 250 m grid scale, the spatiotemporal evolution of ESV and LER in the riparian zone of the Lanzhou–Baiyin metropolitan area (LBMA). The findings reveal concurrent declining trends in both ESV and LER, which signal not ecological improvement but rather systemic degradation towards lower functionality and lower ecological risk. Bivariate LISA clustering was used to identify four categories of ecological regulation zones, offering a spatial foundation for implementing differentiated governance. Building on the four-zone typology, this research further proposes a tiered control strategy encompassing strict protection, urgent restoration, and built-up area optimization, highlighting its advantages compared to conventional single-indicator management. This framework links spatial pattern diagnosis with ecological governance actions and also provides an analytical tool for understanding and managing the security of riparian ecosystems under similar pressures.

Keywords: Yellow River riparian zone; ecosystem service value; landscape ecological risk; spatiotemporal evolution; ecological zoning management

Check for updates

Academic Editors: Brian D. Fath and Wei Song

Received: 3 January 2026
Revised: 2 February 2026
Accepted: 11 February 2026
Published: 13 February 2026

Copyright: © 2026 by the authors. Licensee MDPI, Basel, Switzerland. This article is an open access article distributed under the terms and conditions of the Creative Commons Attribution (CC BY) license.

1. Introduction

As a core engine of regional economic growth, metropolitan areas generate significant polarization and spatial expansion during rapid urbanization. However, this process often disrupts the natural environment and fragments habitats, intensifying the conflict between urban development and ecological conservation [1]. Within this context, the health of the Yellow River, China's second-largest river, is critical to the basin's ecological security and sustainable development [2–4]. The riparian zone, as the primary manifestation of the Yellow River's ecological functions, holds particular importance. This interface acts as a vital transitional area and a final natural barrier for sustaining river health, making it essential for harmonizing the riverine ecosystem with socio-economic needs [5–7]. The

LBMA, located in the upper reaches and serving as the core segment of the Lanzhou–Xining urban agglomeration, epitomizes these challenges [8]. Here, accelerated urbanization has increased anthropogenic pressures on riparian spaces, degrading their ecological integrity. This degradation leads to severe landscape fragmentation and diminished flood control capacity underscore the urgency for action [9]. Therefore, scientific ecological zoning and precise management of these riparian spaces have become urgent prerequisites for sustaining river health and ensuring the region's sustainable development.

As a tier within the ecosystem service cascade framework, ESV, together with LER, assesses regional ecological security and sustainable development, and their integration is crucial for a comprehensive understanding of ecological security. ESV quantifies the economic value of various benefits that ecosystems provide to human society; it measures the stock of ecological capital and the output of service flows, focusing on what ecosystems provide [10,11]. Conversely, LER assesses the potential threats posed by external pressures to landscape structure, function, and processes, often using landscape pattern indices (e.g., fragmentation, isolation) to characterize the vulnerability of the system structure and the likelihood of its degradation, focusing on what ecosystems may lose under stress [12]. Their natures are fundamentally different: ESV reflects the state and supply capacity of functions, whereas LER reveals the stability and latent risks of the system [13,14]. Assessments based exclusively on ESV risk overestimate the safety of ecosystems that currently have high service value but also fragile landscape structures teetering on the brink of decline. Conversely, reliance on LER alone may lead to the misjudgment of areas that, due to intensive artificial management, exhibit homogeneous structures and low risk but have already suffered severe loss of ecological functions. Hence, an integrated and synergistic study of ESV and LER is crucial for achieving a comprehensive grasp of ecosystem conditions and developing effective ecological protection strategies.

Methodologically, both have developed mature quantitative assessment frameworks. For the quantitative calculation of ESV, Xie Gaodi et al. [15] formulated equivalent factors for ecosystem service value per unit area for various land use types in China based on previous studies, thereby determining ecological service values; this method can be widely applied to multi-scale ecosystem research [16–20]. Similarly, LER is also frequently assessed using landscape indices at different scales [12,21–24]. However, existing research still faces several issues. Firstly, a large number of studies have separately investigated either ESV or LER, or have only focused on the impact of land use change on a single indicator, failing to place both within a unified spatial analysis framework [25,26]. Second, an integrated understanding of their driving mechanisms needs further exploration. ESV spatial patterns are typically co-determined by natural and socio-economic drivers [27], whereas LER is strongly associated with anthropogenic disturbances like built-up land expansion [28]. The ways in which these factors interact and propagate spatially to jointly mold the ESV-LER synergy demand further research. Although grid-based analysis has been widely adopted, most studies still focus on the singular description of either ESV or LER. In contrast, bivariate spatial autocorrelation analysis can effectively reveal the spatial relationship between the two, while grid-scale-based analysis can better demonstrate spatial heterogeneity.

Building on these insights, this study develops an integrated spatial-diagnostic framework that couples ESV and LER through bivariate spatial autocorrelation. The framework identifies four distinct spatial relationship types [29,30].

The LBMA serves as a critical economic growth pole within Gansu Province. The Yellow River functions as the region's core water corridor and primary ecological axis, rendering its shoreline space a quintessential ecological-economic ecotone [8]. With the accelerated development of the "Lanbai Economic Zone," rapid urbanization has markedly

intensified anthropogenic pressure on this riparian space. This pressure has progressively eroded the shoreline's ecological attributes, exacerbating landscape fragmentation and compromising the inherent flood control capacity of urban areas. Consequently, the region exemplifies a pronounced conflict between urban expansion and ecological conservation, making it an ideal case for investigating the aforementioned scientific issues [31,32].

Therefore, using the Yellow River riparian zone within the LBMA as an example, this study combines ESV and LER to explore their spatial linkages and synergy at the grid scale. The specific objectives are: (1) to analyze the spatiotemporal evolution patterns of ESV and LER in the rapidly urbanizing upper Yellow River riparian zone and to uncover the drivers behind these patterns; (2) to identify stable spatial-association patterns between ESV and LER using bivariate local spatial autocorrelation and to conduct ecological zoning; and (3) to construct a process-based ecological-zoning framework suitable for linear ecological sensitive zones, thereby overcoming the limitations of traditional management reliant on administrative boundaries or single indicators. This shift from analyzing spatial patterns to formulating operable management strategies offers a foundation for targeted ecological management.

2. Materials and Methods

2.1. The Study Area

The delineation of the study area was primarily informed by the 1 km and 3 km riparian control zones established for different management intensities in the *Yangtze River Economic Belt-Yangtze River Basin Territorial Spatial Plan (2021–2035).* Given the confined valley topography of the upper Yellow River and its intensive human footprint, the spatial context is more compact than that of the middle and lower Yangtze River. Consequently, this study adopts a 2 km buffer—the median value between the two reference zones—as the core research scope. This demarcation is designed to more accurately capture the interaction between human activities and ecological processes within the riparian zone of a valley city.

Situated in a critical section of the upper Yellow River, the LBMA serves as a central pillar for economic growth and a hub of economic activity in Gansu Province, holding significant geographical and ecological importance [33]. Within the study area, the main stem of the Yellow River stretches 450.53 km from west to east, forming an ecological corridor and an urban–rural development axis across central Gansu [34,35]. Its riparian space represents a typical composite ecosystem and an eco-economic transition zone. The landforms along the river encompass the Loess Plateau, gorges, and sections of alluvial plains, featuring diverse geomorphic types that give rise to a unique ecosystem (Figure 1). The region experiences a continental monsoon climate, featuring cold, arid winters and hot, wet summers. Low and uneven rainfall results in an unreliable water supply and concurrent drought-flood hazards, thereby heightening the ecosystem's sensitivity and fragility. In contrast to plain cities, urban sprawl here is severely limited by the confined valley terrain, leading to a linear, corridor-like pattern of encroachment following the river and key transport lines. This intensifies the fragmentation of ecological land uses like cropland and woodland, establishing a pronounced human pressure–ecological response gradient. Therefore, this region serves as a typical example for investigating the evolution patterns of landscape ecological risk and ecosystem service value in riparian spaces under the interaction of intensive human activities and a fragile ecological environment [23].

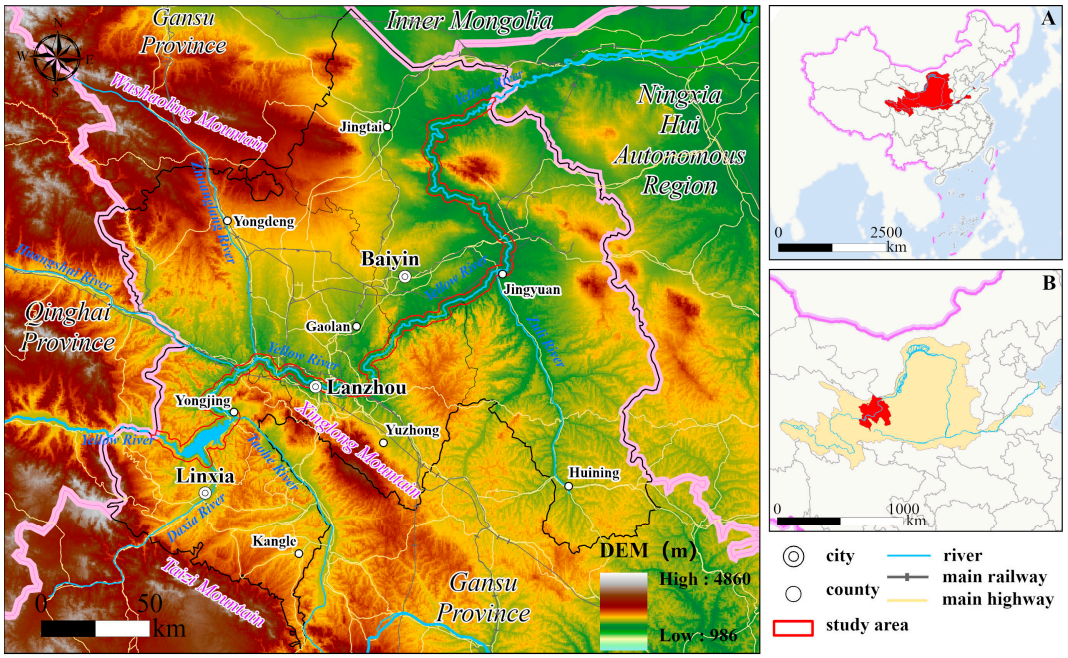


Figure 1. Location map of the study area. (**A**) Location of the Yellow River Basin in China, (**B**) Location of the LBMA in the Yellow River Basin, (**C**) Location of the study area in LBMA. Map content approval number is GS (2020)4619. The administrative boundaries are shown as per this source and have not been altered.

2.2. Data Sources and Preprocessing

This study utilizes multi-source data from four time points (1990, 2000, 2010, and 2020), including fundamental geographic data, remote sensing imagery, and socio-economic statistics. All data were standardized to the CGCS2000 geographic coordinate system. Land Use and Cover Change (LUCC) data were obtained from the authoritative Chinese multi-period land use remote sensing monitoring dataset, which classifies land into six categories: cultivated land, forest land, grassland, water, construction land, and unused land. The dataset was produced through human–computer interactive visual interpretation, using primary imagery from the Landsat series (Landsat MSS, TM/ETM+, and Landsat 8). Subsequent area calculations are based on 30 m resolution raster data. It is important to note that while the numerical results are derived from pixel-counting algorithms, the spatial recognition accuracy is constrained by the 30 m pixel scale. Consequently, all area analyses reflect macro-level land use change trends within the region. Detailed data sources and descriptions are provided in Table 1.

Table 1. Data source.

Data Types	Data Name	Data Source	Data Format
Fundamental Geographic Data	Administrative boundaries of the study area	Standard map service system (http://bzdt.ch.mnr.gov.cn/) accessed on 5 June 2025	Shp
Remote sensing satellite monitoring data	Land use and cover change	Resource and Environmental Science Data Platform (https://www.resdc.cn/) accessed on 8 June 2025	Raster (30 m)
Road network data	Railway, highway network data	OpenStreetMap (https://www.openstreetmap.org) accessed on 15 August 2025	Shp
Socio-economic data	Total sown area Total grain output The price of grain	National Bureau of Statistics (https://www.stats.gov.cn) accessed on 2 September 2025 Gansu Provincial Bureau of Statistics (https://tjj.gansu.gov.cn) accessed on 22 September 2025	Excel

2.3. Methods

Based on land use data, the study area was divided into 250 m × 250 m grid units. While spatiotemporal analysis of LUCC can reveal evolutionary patterns, it does not sufficiently quantify the gains and losses and spatial interactions of multiple ecosystem functions. To address this, we assessed ESV to quantify the service functions of different land types, calculated landscape indices using Fragstats 4.2 to construct a composite LER index, providing a comprehensive reflection of regional ecological security. Subsequently, bivariate spatial autocorrelation analysis was employed to identify spatial clustering patterns and synergistic relationships between ESV and LER. Based on these results, an ecological zoning model was developed, dividing the study area into four typical ecological control zones, for which tailored optimization strategies were proposed (Figure 2).

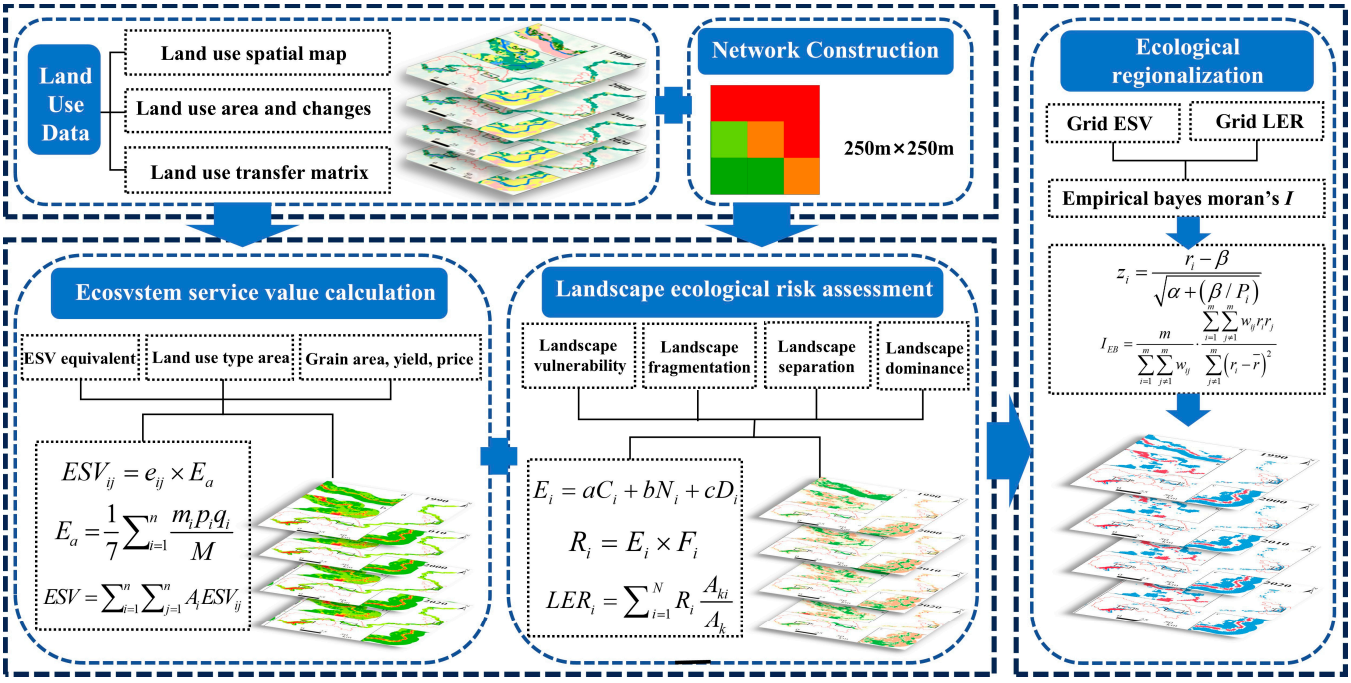


Figure 2. Technical Roadmap.

2.3.1. Division of Research Units

Using ArcGIS Pro 3.4 software, the river shoreline space was segmented at equal intervals. To examine the effect of grid scale, we compared the analytical results at scales of 1000 m, 500 m, and 250 m. Considering computational intensity, accuracy, and the actual conditions of the study area comprehensively, a 250 m × 250 m grid was ultimately selected as the assessment unit, resulting in a total of 33,682 grids. Each grid served as an ecological research unit for spatial sampling and calculation (Figures S1–S3) [36].

2.3.2. ESV Estimation

For the ESV assessment, this study applied the unit area value equivalent system developed by Xie Gaodi et al. [15]. This system employs a unified value equivalent factor to enable the dynamic quantitative assessment of 11 service functions across 14 ecosystem types in China, providing a robust methodological foundation for regional value accounting [37,38]. The six land use categories in this study were mapped to corresponding ecosystem types from the benchmark table. This adaptation produced a modified equivalent value table tailored to the local context (Table 2).

Table 2. ESV equivalents for riparian areas along the main stream of the Yellow River in the LBMA.

Ecosystem Service Function	Cultivated Land	Forest Land	Grassland	Waters	Construction Land	Unused Land
Food Production	0.85	0.25	0.23	0.80	0.00	0.01
Production of material	0.40	0.58	0.34	0.23	0.00	0.03
Water supply	0.02	0.30	0.19	8.29	0.00	0.02
Gas conditioning	0.67	1.91	1.21	0.77	0.00	0.11
Climate regulation	0.36	5.71	3.19	2.29	0.00	0.10
Environmental purification	0.10	1.67	1.05	5.55	0.00	0.31
Hydrological regulation	0.27	3.74	2.34	102.24	0.00	0.21
Soil conservation	1.03	2.32	1.47	0.93	0.00	0.13
Maintain nutrient cycle	0.12	0.18	0.11	0.07	0.00	0.01
Bio-diversity	0.13	2.12	1.34	2.25	0.00	0.12
Aesthetic landscape	0.06	0.993	0.59	1.89	0.00	0.05
Total	4.01	19.77	12.06	125.31	0.00	1.10

Based on the established ratio that the output value of grain crops per unit area represents seven times the economic value of ecosystem services, a calculation was performed using regional agricultural data. According to the *Gansu Statistical Yearbook*, the total grain output is predominantly wheat. The average grain yield from 1990 to 2020 was calculated as 3202.27 kg·hm^{-2}, with a staple food market price of 2.3 CNY·kg^{-1} and an average cultivated area of 2.75 × 10^6 hm^2. Substituting these values into Equation (1), the economic value coefficient per unit ecosystem service value equivalent for the study area was determined to be 1043.03 CNY·hm^{-2}.

$$E_a = \frac{1}{7}\sum_{i=1}^{n} \frac{m_i p_i q_i}{M} \quad (1)$$

where E_a is the economic value coefficient of ESV equivalent in the study area (CNY·hm^{-2}); m_i is the planting area of crops in the study area (hm^2); p_i is the average grain price (CNY·kg) in Gansu Province from 1990 to 2020; q_i is the average grain yield (kg·hm^{-2}) in the study area from 1990 to 2020; M is the total area of crops planted in the study area (hm^2).

Using the established ESV equivalent and the regional economic value coefficient, the ESV per unit area was calculated according to Equation (2). This yielded the value coefficients per unit area for 11 ecosystem service functions within the buffer zone and for the six land use types, as detailed in Table 3.

$$ESV_{ij} = e_{ij} \times E_a \quad (2)$$

where i is the type of land use; j is the type of ecosystem service function; ESV_{ij} is the corresponding ecosystem service value per unit area; e_{ij} is the ESV equivalent corresponding to the ecosystem service function of land type; E_a is the economic value coefficient of ESV equivalent in the study area.

Table 3. ESV per unit area for riparian areas along the main stream of the Yellow River in the LBMA. (CNY·hm^{-2}).

Ecosystem Service Function	Cultivated Land	Forest Land	Grassland	Waters	Construction Land	Unused Land
Food Production	886.57	260.76	239.90	834.42	0.00	10.43
Production of material	417.21	604.96	354.63	239.90	0.00	31.29
Water supply	20.86	312.91	198.18	8646.69	0.00	20.86
Gas conditioning	698.83	1992.18	1262.06	803.13	0.00	114.73

Table 3. *Cont.*

Ecosystem Service Function	Cultivated Land	Forest Land	Grassland	Waters	Construction Land	Unused Land
Climate regulation	375.49	5955.68	3327.25	2388.53	0.00	104.30
Environmental purification	104.30	1741.85	1095.18	5788.80	0.00	323.34
Hydrological regulation	281.62	3900.92	2440.68	106,639.03	0.00	219.04
Soil conservation	1074.32	2419.82	1533.25	970.01	0.00	135.59
Maintain nutrient cycle	125.16	187.74	114.73	73.01	0.00	10.43
Bio-diversity	135.59	2211.22	1397.66	2346.81	0.00	125.16
Aesthetic landscape	62.58	1035.73	615.39	1971.32	0.00	52.15
Total	4182.54	20,623.76	12,578.90	130,701.65	0.00	1147.33

The total ESV of the Yellow River riparian zone in the LBMA from 1990 to 2020 was calculated using Equation (3).

$$ESV = \sum_{i=1}^{n} \sum_{j=1}^{n} A_i ESV_{ij} \quad (3)$$

where i is the type of land use; j is the type of ecosystem service function; ESV is the value of ecosystem services in the study area; A_i is the area of class i land; ESV_{ij} is the corresponding ecosystem service value per unit area.

2.3.3. Construction of LER Index

ArcGIS Pro, Fragstat 4.2 and Excel 2019 were used to calculate the fragmentation, separation and dominance of a single grid, and the interference degree was calculated by weighting superposition. Combined with the landscape interference degree (E_i) and landscape vulnerability (F_i) index, the landscape loss degree (R_i) was calculated to further calculate the landscape ecological risk in a single grid. Based on the LER range of different periods and different scenarios, the LER was divided into highest-risk area, high-risk area, moderate-risk area, low-risk area and lowest-risk area by equal interval method. The calculation formula is as follows:

$$E_i = aC_i + bN_i + cD_i \quad (4)$$

where E_i is landscape disturbance; C_i is landscape fragmentation index; N_i is landscape separation index; D_i is the landscape advantage index; a, b, c are the weights of C_i, N_i and D_i, respectively, and $a + b + c = 1$; referring to previous studies, the weights of a, b and c are assigned 0.5, 0.3 and 0.2 respectively [39–41].

$$C_i = \frac{n_i}{A_i} \quad (5)$$

where A_i is the total area of land use type i; n_i is the number of patches of land use type i.

$$S_i = \frac{A}{2A_i}\sqrt{\frac{N_i}{A}} \quad (6)$$

where A is the total area of the study area.

$$D_i = \frac{Q_i + M_i}{4} + \frac{L_i}{2} \quad (7)$$

where Qi is the proportion of the number of squares appearing in the patch to the total number of squares, M_i is the proportion of the number of patches i to the total number of patches, and L_i is the proportion of the area of patches to the total area of the sample.

$$R_i = E_i \times F_i \tag{8}$$

where R_i is landscape loss; E_i is the degree of landscape disturbance of type i; F_i is the vulnerability index of class i landscape.

Based on previous studies [39–41], the vulnerability of the six land use types was assessed using the previous research results. The resulting F_i for each landscape type was then normalized (Table 4).

Table 4. Landscape vulnerability index.

Landscape Type	Cultivated Land	Forest Land	Grassland	Waters	Construction Land	Unused Land
Value	4	3	2	5	1	6
Vulnerability index	0.190	0.095	0.143	0.238	0.048	0.286

Finally, the LER is calculated by Equation (9).

$$LER_i = \sum_{i=1}^{N} R_i \frac{A_{ki}}{A_k} \tag{9}$$

where LER_i is the i the ecological risk index of risk area. A_{ki} is the area of the first type of landscape in the kth risk community: A_k is the area of the kth risk community; R_i is the landscape loss index of the first type of landscape.

2.3.4. Ecological Zoning Model Based on ESV and LER

Building on the ESV and LER indices, the spatial agglomeration between them was analyzed using both global and local Moran's *I*. To address potential statistical bias caused by variance nonstationarity in the original data, the Empirical Bayes (EB) standardization method proposed by Assunção et al. [42] was employed. This method corrects Moran's *I* statistics for varying population densities across observational units. Accordingly, this study introduces the Empirical Bayes Moran's *I* (I_{eb}), which smooths local variance through Bayesian shrinkage estimation, to comprehensively evaluate the synergistic and differentiated spatial relationship between ESV and LER [43,44]. The calculation is defined as follows:

$$z_i = \frac{r_i - \beta}{\sqrt{\alpha + (\beta / P_i)}} \tag{10}$$

$$I_{EB} = \frac{m}{\sum_{i=1}^{m} \sum_{j \neq 1}^{m} w_{ij}} \cdot \frac{\sum_{i=1}^{m} \sum_{j \neq 1}^{m} w_{ij} r_i r_j}{\sum_{j \neq 1}^{m} (r_i - \bar{r})^2} \tag{11}$$

where i and j are the evaluation units, z_i is the standardized value of r_i, r_i is the ratio of ESV to LER in the unit, I_{EB} is the bivariate empirical Bayesian global autocorrelation coefficient of ESV per unit area and LER, m is the number of grids in the study area, w_{ij} is the weight value between i and j, and $\bar{r}$ is the average value of r_i.

3. Results

3.1. Spatiotemporal Changes in LUCC

3.1.1. LUCC Temporal Variation

Table 5 shows the land area changes from 1990 to 2020, and Figure 3 visualizes the area transfers between different land use types at four time points. The arrow widths correspond to the extent of area conversion, and together they elucidate the transformation

in land structure. The distinct valley terrain and fragile ecosystem in the upper Yellow River region give rise to a unique, locally specific transformation pathway. In contrast to the widespread expansion typical of cities on plains, urban development in this area is limited by the scarce flat land within the valley, leading to a more focused and linear pattern of encroachment along the riparian corridor. The most prominent trend is the continuous expansion of construction land, which increased by a net total of 6915.96 hm^2 over the thirty-year period. This trend indicates that urbanization in the study area occurred largely at the expense of ecological and agricultural land. In contrast, ecologically productive land—cultivated land, forest land, and grassland—declined, creating a clear divergence in land use trajectories.

Table 5. LUCC area change in the Yellow River main stream riparian zone in LBMA. (hm^2).

LUCC Types	1990–2000	2000–2010	2010–2020	1990–2020
Cultivated land	−1064.34	86.76	−3088.08	−4065.66
Forest land	2.34	−952.29	−411.57	−1361.52
Grassland	−189.99	−677.16	−185.13	−1052.28
Waters	−99.27	−624.42	390.87	−332.82
Construction land	1356.12	1896.12	3663.72	6915.96
Unused land	−4.86	274.95	−288.36	−18.27

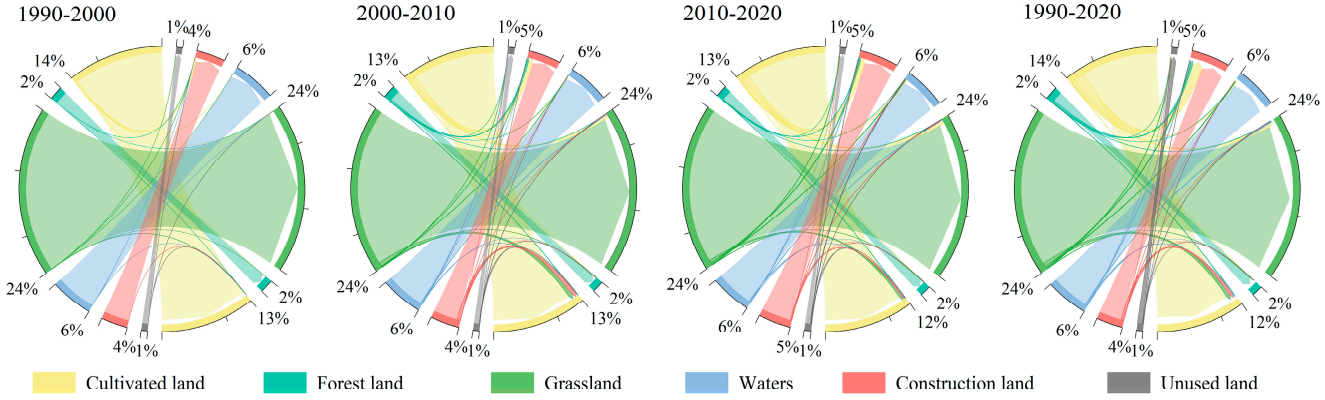


Figure 3. LUCC of riparian zone in the main stream of the Yellow River in LBMA from 1990 to 2020.

The period can be divided into three distinct stages:

1990–2000 (Initial Stage): Construction land increased by 1356.12 hm^2, while cultivated land decreased by 1064.34 hm^2, marking the initial substitution of agricultural space by urban and rural development. Concurrent reductions in grassland and water signify the early encroachment of human activity into natural ecological spaces. 2000–2010 (Acceleration Stage): The pace of change intensified and diffused. The expansion of construction land rose to 1896.12 hm^2, accompanied by a significant decrease in forest land, reflecting a pronounced erosion of ecological space by urbanization. The accelerated shrinkage of water area during this stage suggests that pressure on regional water resources and ecosystems peaked. 2010–2020 (Intensification Stage): Changes were most dramatic. Urban and rural construction land grew explosively, while cultivated land experienced its most significant reduction over the entire study period, highlighting an acute conflict between land urbanization and agricultural protection. Notably, water area achieved reversible growth in this stage, reflecting the positive impact of ecological management measures.

Land use change in the study area exhibits distinct stage-specific characteristics, which in essence reflect a continuous process of urban space encroaching upon ecological and agricultural spaces. Under the context of rapid urbanization, human–land relations in the

LBMA are growing tense, making the coordination of urban development and ecological conservation a central challenge ahead.

3.1.2. LUCC Spatial Variation

Figure 4 displays the spatial distribution of six land use types across four temporal slices. The visualization zooms in on three urban areas, revealing that cultivated land in the study area is mainly located in extensive, contiguous tracts, especially near rivers and in the periphery of urban regions. Construction land expansion is heavily concentrated on the limited plains within river valleys and along key transport corridors. This results in the consumption of highly productive ecological land, especially cropland and forestland. This pattern causes pronounced linear fragmentation of the riparian landscape, threatening ecological connectivity in critical areas. Grassland is chiefly located in peri-urban transitional areas, while construction land exhibits a more concentrated spatial pattern. An inset map details the development of three focal regions:

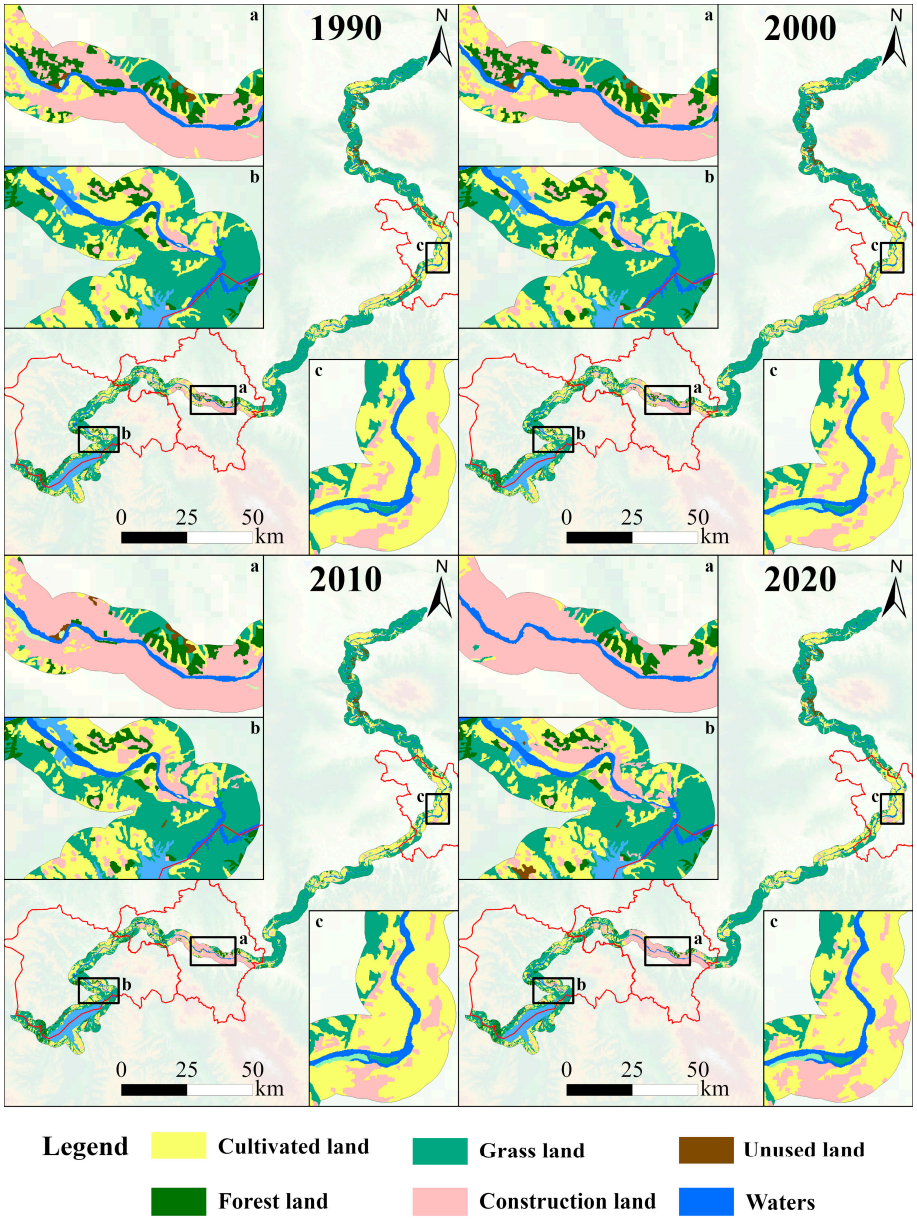


Figure 4. The spatial and temporal transformation characteristics of LUCC in the main stream of the Yellow River in LBMA from 1990 to 2020.

Region a comprises the central urban area of Lanzhou (LZC), where construction land is heavily concentrated. As the provincial capital core, this region has benefited from substantial policy support and resource allocation, linking its urbanization directly to national macro-strategies promoting urban expansion and economic growth. Regions b and c are the central urban areas of Yongjing (YJC) and Jingyuan (JYC) counties, respectively. These county-level cities are situated along the Yellow River's main stream, relying on relatively flat floodplains and terraces for development. The two cities share generally consistent overall development trajectories and features, with 2010 serving as a turning point for major transformations. Development prior to 2010 was relatively stable, characterized by slower urbanization and less land-use change. At that time, under China's Western Development Strategy, emphasis was placed on infrastructure construction and ecological conservation in western regions, which helped preserve the original land-use patterns of the towns to a certain extent.

3.2. Spatiotemporal Changes in ESV

3.2.1. ESV Temporal Variation

Based on the land use change analysis from 1990 to 2020, the ESV for each land category was further assessed (Table 6). Overall, the total ESV in the study area followed a pattern of overall decline, local fluctuation, and recent stabilization, indicating a general degradation of ecosystem service functions with some positive signs of recovery in the later period. From 1990 to 2000, total ESV decreased slowly by 0.20×10^6 CNY. Apart from forest land, which remained relatively stable, the ESV of key ecological land types, including cultivated land, grassland, and water bodies, experienced a mild decrease, suggesting nascent pressure from human activities on the ecosystem during this phase, albeit not intense. The period from 2000 to 2010 witnessed a sharp decline in ESV, with the total value decreasing by 1.09×10^6 CNY, representing a significantly expanded rate of reduction. In this stage, the ESV of water bodies declined the most, accompanied by notable degradation of forest land, mirroring the intense disruption inflicted by rapid urbanization and land-use alterations on water and forest ecosystems. A structural turnaround occurred from 2010 to 2020, with the total ESV increasing instead of decreasing, rising by 0.27×10^6 CNY. The ESV of water bodies notably recovered, becoming a key driver of the overall value rebound, likely attributable to the implementation of ecological restoration and water resource management policies; however, the ESV of cultivated land and forest land continued to decline, indicating ongoing pressure on the recovery of their ecological functions.

Table 6. ESV and ESV variation in the Yellow River mainstream riparian zone in the LBMA. (10^6 CNY).

Year	1990	2000	2010	2020	1990–2000	2000–2010	2010–2020	1990–2020
Cultivated land	2.23	2.18	2.19	2.06	−0.0445	0.0036	−0.1292	−0.1700
Forest land	1.57	1.57	1.37	1.29	0.0005	−0.1964	−0.0849	−0.2808
Grassland	11.88	11.86	11.77	11.75	−0.0239	−0.0852	−0.0233	−0.1324
Waters	31.01	30.88	30.06	30.57	−0.1297	−0.8161	0.5109	−0.4350
Unused land	0.04	0.04	0.04	0.04	−0.0001	0.0032	−0.0033	−0.0002
Total	46.73	46.53	45.44	45.71	−0.1977	−1.0909	0.2702	−1.0184

In summary, the ecosystem service value of the Yellow River shoreline in the LBMA experienced a net decline over the past three decades, with a cumulative decrease of 1.02×10^6 CNY. The most severe degradation occurred between 2000 and 2010. Although the recovery of aquatic ecological functions from 2010 to 2020 contributed to an overall ESV rebound, the persistent declines in other land types underscore the continued need for

ecological protection and restoration aimed at enhancing overall ecosystem quality and structural stability.

3.2.2. ESV Spatial Variation

In this study, the Natural Breaks method was used to classify and visualize the ESV across grid units. Figure 5 shows the ESV levels of the riparian zone across four time periods, with ESV classified into five grades: highest ($\geq$6.80 $\times$ 10^6 CNY), high (6.80 $\times$ 10^6–4.30 $\times$ 10^6 CNY), medium (4.30 $\times$ 10^6–1.95 $\times$ 10^6 CNY), low (1.95 $\times$ 10^6–0.56 $\times$ 10^6 CNY), and lowest (<0.56 $\times$ 10^6 CNY). Spatially, the highest ESV areas correspond predominantly to water bodies, extending in a west–east linear pattern along the Yellow River corridor. High and medium-value zones are largely distributed in proximity to these aquatic features, exhibiting a degree of spatial clustering. The lowest-value class occupies the largest share of the study area and is concentrated around built-up peripheries, while low-value areas generally coincide with transitional zones between urban and natural ecosystems.

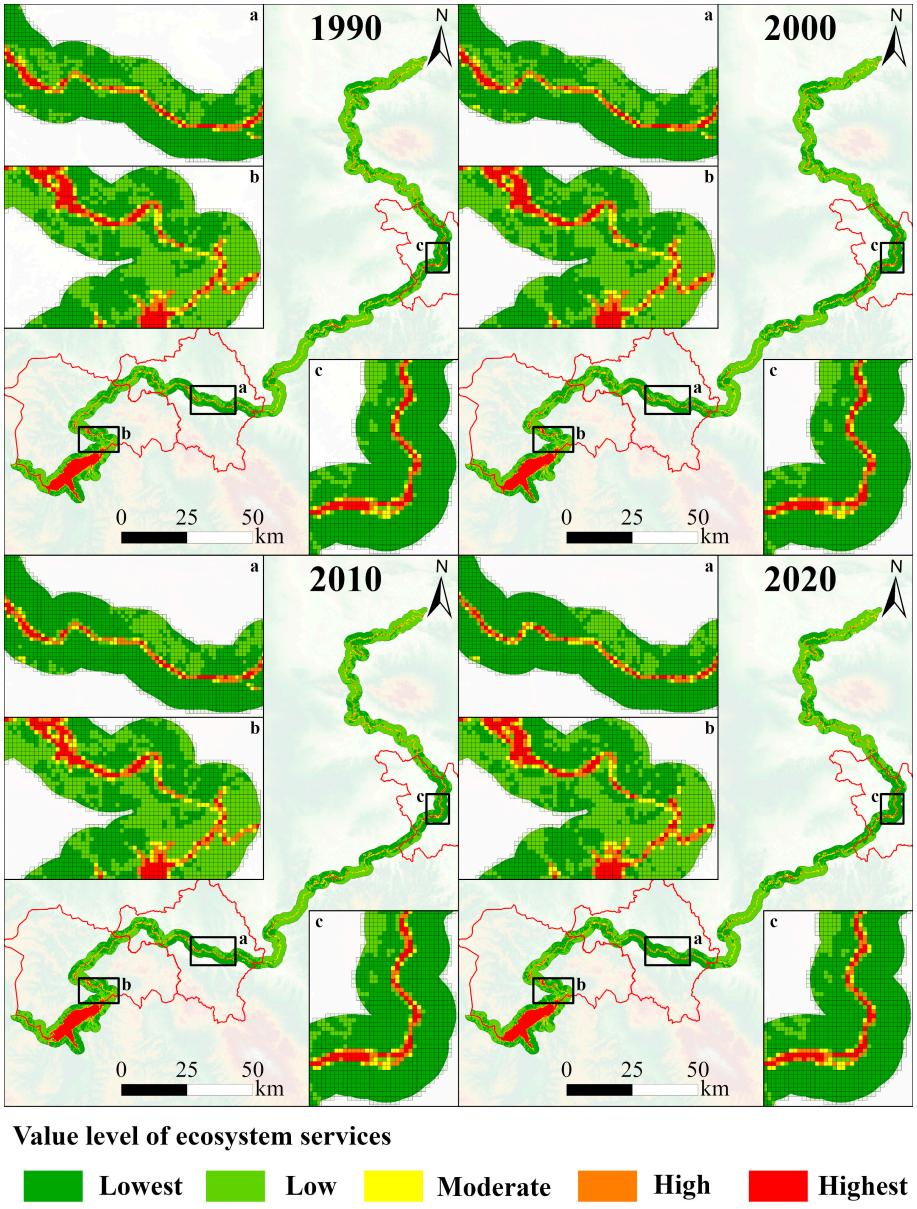


Figure 5. The spatial and temporal transformation characteristics of ESV in the riparian zone of the main stream of the Yellow River in LBMA from 1990 to 2020.

In the LZC area, the lowest ESV class predominates. Driven by rapid urban sprawl, extensive riverfront areas have been progressively converted to built-up land. The intense land-use alteration has markedly degraded ecosystem service provision, resulting in the ongoing enlargement of areas with low ESV. The YJC and JYC areas are dominated by low ESV classes. Despite noticeable urbanization, the region's overall ecosystem service provisioning capacity remains weak due to the combined influence of predominant traditional farming, low vegetation cover, and water shortages, which is reflected in the extensive distribution of low-value zones.

3.3. Spatiotemporal Changes in LER

3.3.1. LER Temporal Variation

Employing a landscape ecological index methodology, data for each land category in the study area were calculated. The comprehensive LER indices for 1990, 2000, 2010, and 2020 were 0.015128, 0.015305, 0.014875, and 0.014841, respectively. Although minor fluctuations are present, the LER demonstrates a general downward trend, suggesting a stabilization and slight optimization of the risk-level structure and an alleviation of landscape pattern structural risk in the region. Using the natural breaks method, LER values were classified into five categories: lowest risk (LER < 0.010136), low risk ($0.010136 \leq$ LER < 0.013277), medium risk ($0.013277 \leq$ LER < 0.016102), high risk ($0.016102 \leq$ LER < 0.028068), and highest risk (LER $\geq$ 0.028068). The changes in area and proportional share for each risk category were subsequently calculated (Table 7).

Table 7. LER and LER changes in various types of riparian zones in the main stream of the Yellow River in LBMA from 1990 to 2020.

Ecological Risk Level	Area (hm^2)				Proportion (%)			
	1990	2000	2010	2020	1990	2000	2010	2020
Lowest	27,687.5	38,512.5	30,425	35,687.5	13.17	18.32	14.47	16.97
Low	16,437.5	12,437.5	15,356.25	15,106.25	7.82	5.92	7.30	7.18
Moderate	110,593.75	106,081.25	107,775	107,900	52.60	50.45	51.26	51.32
High	50,275	47,968.75	51,462.5	46,631.25	23.91	22.81	24.48	22.18
Highest	5268.75	5268.75	5243.75	4937.5	2.51	2.51	2.49	2.35

A comprehensive analysis reveals that ecological risk in the study area is consistently dominated by the medium-risk level, which maintained an area proportion exceeding 50% throughout the study period, reflecting a generally stable regional risk pattern. The lowest-risk area exhibited a fluctuating upward trend, increasing from 13.17% in 1990 to 16.97% in 2020, indicating an improvement in ecological conditions in some locations, possibly due to concentrated conservation measures. The high-risk area showed an overall decline from 23.91% to 22.18%, despite a temporary rebound in 2010 that may be linked to intensified land-use conversion during that interval. Meanwhile, the proportion of the highest-risk category continued a gradual decline, suggesting that areas of extreme ecological risk are being brought under control. Overall, despite periodic fluctuations, the landscape ecological risk structure in the study area has trended toward stability and slight optimization over the 30-year period. The combined share of medium- and higher-risk zones has decreased, while the lowest-risk area has expanded considerably. This indicates that the region retains a degree of ecological resilience even amidst rapid urbanization.

3.3.2. LER Spatial Change

Figure 6 shows the LER levels of the riparian zone across four time periods, with LER classified into five grades. The figure reveals a pattern generally dominated by

medium-risk levels. These areas are widely distributed within the ecological transition zones between urban centers, reflecting the typical risk profile of such interfaces under pressure from land use conversion and human activity. Low-risk areas are predominantly concentrated along the river shoreline and adjacent waters near Lanzhou City, a pattern likely attributable to systematic ecological protection and planning controls in these zones. The water body itself, acting as a landscape matrix, also helps mitigate ecological risk in its vicinity. In contrast, most other built-up areas exhibit high-risk levels, indicative of the natural landscape fragmentation and decline in ecosystem services that commonly accompany urban expansion. The highest-risk areas are scattered sporadically throughout the study area.

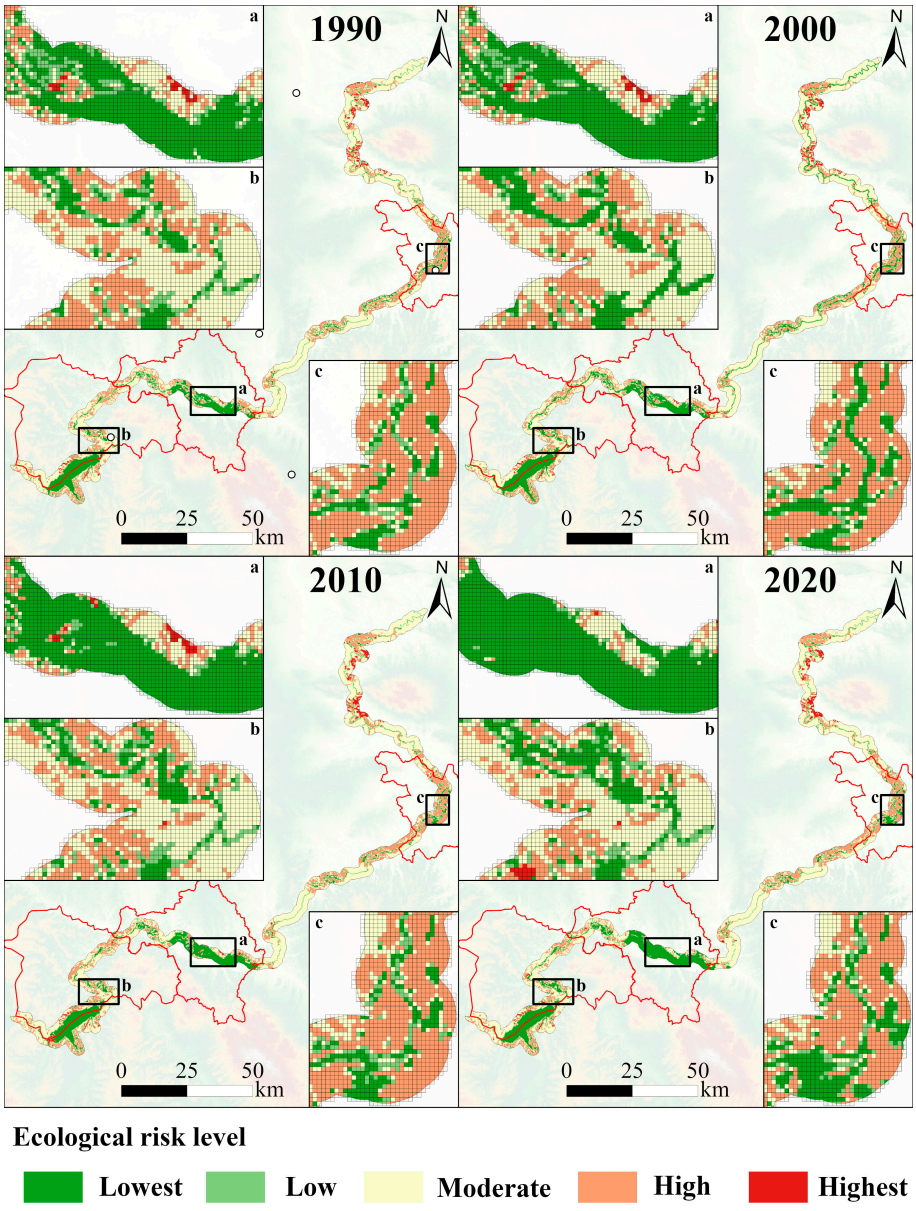


Figure 6. The spatial-temporal transformation characteristics of LER in the main stream of the Yellow River in LBMA from 1990 to 2020.

The LER in the LZC remains at a low level. As a highly urbanized built-up area, it has seen strengthened governmental monitoring and management of the urban ecological environment in response to development-related environmental pressures. Although construction land expansion has encroached on pre-existing green spaces and natural

landscape elements have largely disappeared, this very loss has reduced the potential for sudden environmental risks arising from fluctuations in natural ecosystems, thereby lowering the landscape ecological risk index to some degree. The YJC region is mainly composed of moderate-to-high risk levels. Developed based on the Liujiaxia Reservoir, this emerging town's rapid tourism and related infrastructure development have driven built-up land expansion and natural landscape alteration. This has disrupted the original eco-landscape structure, increased landscape fragmentation, and reduced ecosystem stability, thereby sustaining a relatively high LER in the region. The development pattern of JYC is partly shaped by national agricultural support policies. To safeguard grain production and stable agricultural development, the region retains a high proportion of farmland. Intensive agricultural practices and associated water resource regulation and use are probable significant drivers behind its consistently elevated ecological risk. This phenomenon indicates that even in areas with relatively slow urbanization, the continuous pressure of human activities on ecosystems cannot be overlooked.

3.4. Construction of Ecological Zoning Model Based on EBI

Employing bivariate local spatial autocorrelation analysis (Equations (10) and (11)), the relationship between ESV and LER was examined, yielding distinct spatial clustering patterns. The empirical Bayesian-adjusted bivariate global Moran's I for ESV and LER from 1990 to 2020 was calculated as 0.763, 0.768, 0.841, and 0.754, respectively, indicating a consistently significant positive spatial correlation between the two variables. The Moran scatter plot (Figure 7) delineates four types of local spatial associations. Furthermore, A bivariate LISA cluster map (Figure 8) was generated to visualize these agglomeration patterns, which exhibit clear spatial differentiation.

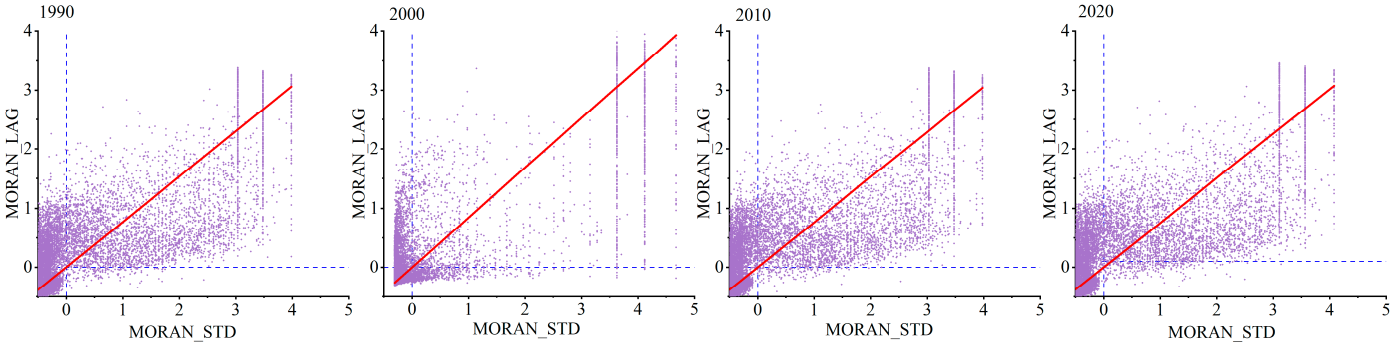


Figure 7. Moran scatter plot of spatial ecological zoning of riparian zone in the main stream of the Yellow River in LBMA from 1990 to 2020.

High–High Agglomeration (High ESV–High LER): Represents ecological "highlands under pressure". These areas possess a strong ecological baseline and high service capacity but are encircled by environments with high ecological risk. Management should prioritize strict protection against over-exploitation and enhance the restoration of natural resources.

High–Low Agglomeration (High ESV–Low LER): Reflects an ideal synergy, where high ecosystem function coexists with a low-risk environment. This pattern suggests successful integration of ecological protection and regional development policies. Its limited occurrence in the study area, however, indicates that a systematic "high-security–low-risk" synergy is not yet widespread, highlighting the need to strengthen coordinated mechanisms for ecological protection and risk mitigation.

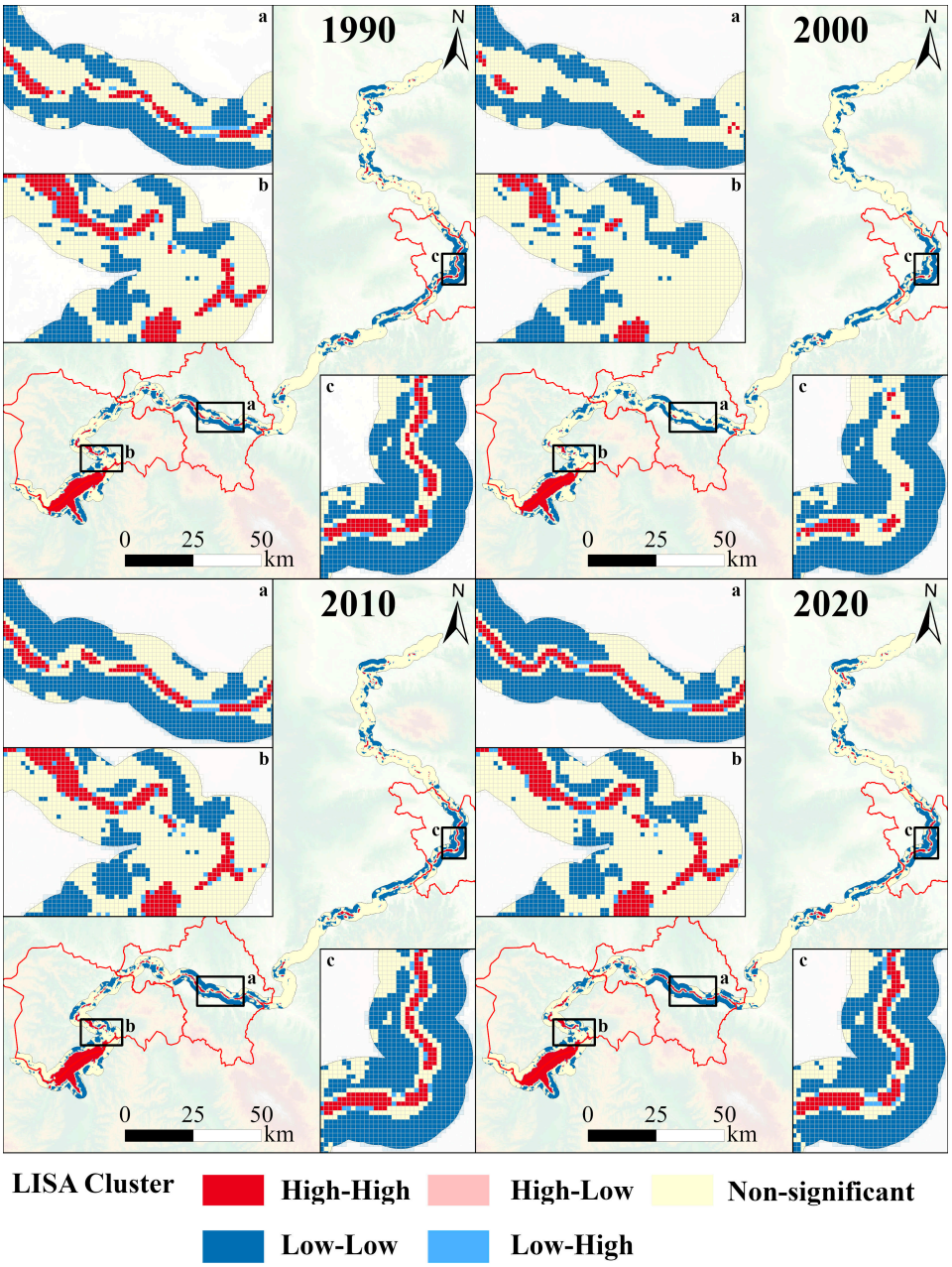


Figure 8. LISA cluster analysis map of riparian zone of the Yellow River mainstream in LBMA from 1990 to 2020.

Low–Low Agglomeration (Low ESV–Low LER): Characterizes areas with modest ecosystem service value and relatively low ecological risk, typically found in highly urbanized zones. Although the inherent ecological background is weak, standardized land-use planning and control measures appear to have contained the accumulation of ecological risk.

Low–High Agglomeration (Low ESV–High LER): Corresponds to a "risk-depression" contradiction, where a core area with degraded ecological function is surrounded by high-risk sources. This sporadic pattern signals a severe spatial mismatch between ecological function and risk level, marking these zones as critical targets for ecological restoration and risk-source remediation.

4. Discussion

4.1. Analysis of Spatiotemporal Drivers of ESV and LER

The study revealed the spatiotemporal evolution characteristics of ESV and LER in the riparian zone of the LBMA and identified their interrelated evolutionary mechanisms. Firstly, policy drivers and topographic constraints jointly shaped the mechanism of phased linear encroachment in land use evolution. Land use changes indicate that construction land expansion was not uniform but exhibited a phased characteristic of "slow growth–acceleration–sharp surge" during the study period [45]. This phasing closely aligns with policy milestones such as the deepening of the national "Western Development" strategy and the launch of the local "Lanzhou–Baiyin Economic Zone" plan, indicating that macro-level policies are key external drivers of land use transformation [46,47]. Unlike the sprawling expansion pattern of plain cities, construction land expansion in the study area did not form a sprawl pattern but, constrained by the valley topography, extended along the main channel of the Yellow River and major transportation arteries as a "linear corridor". Consequently, ecologically valuable cropland and forest land have been fragmented and consumed [48].

Second, the co-decline of ESV and LER reveals a progression toward a "low-functionality, low-disturbance" steady state. Time-series analysis shows that over the 30 years, the regional ESV net decreased by 1.02×10^6 RMB, and the composite LER index also dropped from 0.015128 to 0.014841. The persistent decline in ESV, particularly the loss of value from farmland and forest land, directly reflects the irreversible replacement of ecological capital by construction land [49,50]. Meanwhile, the decrease in LER is largely attributable to a fundamental shift in landscape structure within highly urbanized zones. The landscape in these areas has transitioned from natural patches to large-scale, homogeneous impervious surfaces. LER, calculated based on landscape pattern indices, quantifies structural sensitivity to land use change; when natural patches nearly vanish, the risk generated by rapid land use conversion also diminishes, entering a human-management-dominated equilibrium state, which is why highly urbanized areas exhibit lower or moderate risk levels [51,52]. This finding challenges the conventional assumption that a decline in LER signifies ecological improvement. Instead, in intensely urbanized riparian zones, it may signal the completion of a transition to a human-controlled, ecologically impoverished state, a nuance often overlooked in studies focusing solely on LER trends.

In summary, this study finds that in the riparian space of an upstream valley-type metropolitan area, due to topographic constraints and policy-driven encroachment on natural space, the riparian ecosystem undergoes a specific degradation process from dynamic loss to a static, low steady state [53,54].

4.2. Methodological Evaluation: Efficacy and Boundaries of the Integrated Zoning Framework

A core contribution of this study is the development and application of an integrated ESV-LER-Bivariate Spatial Autocorrelation framework for ecological zoning. This framework advances the field by moving beyond isolated assessments [55,56] to provide a spatially explicit diagnosis of the synergies and trade-offs between ESV and LER.

Unlike traditional single-indicator zoning methods, the framework presented in this paper addresses the spatial mismatch between ecosystem function and structural stability [57,58]. This diagnostic approach overcomes the limitations of traditional methods, which can yield misleading assessments when high service provision coexists with potential instability, or when a low-risk indicator masks functional degradation [59]. To this end, the study employs a bivariate LISA based on Moran's I and adjusted using the Empirical Bayes method. This identifies spatial clusters at the critical intersections of ESV

and LER patterns. The Empirical Bayes adjustment corrects for variance instability among observational units, ensuring a more robust identification of significant clusters.

This integrated framework utilizes analysis units based on natural processes to provide policy-relevant spatial patterns. The framework offers an advantage over traditional zoning, which relies merely on land use or a single ecological metric, by clearly revealing the spatial coupling of function and risk and pinpointing priority zones where management interventions could yield co-benefits for ESV and LER. First, the framework defines a 2 km study buffer zone, aligned with management intensity zoning for riparian control, reflecting the focused nature of human–environment interactions in arid valley cities. Second, a 250 m grid is employed as the fundamental evaluation unit. This scale sufficiently reveals the fragmented patterns and gradient features of the urban-agricultural-ecological ecotone, effectively balancing the "identification of ecological process continuity" with the "practical operability of regional management." The zoning results reflect the intrinsic continuity of riparian ecological processes. This is crucial for managing linear corridors like riverbanks, as ecological functions and risks transcend administrative boundaries.

However, a critical evaluation necessitates a clear delineation of the framework's inherent boundaries and limitations. The model excels at revealing the spatial patterns of ESV-LER relationships but, on its own, fails to elucidate the underlying socio-ecological processes or predict future states under different scenarios. The ESV assessment relies on static value equivalence factors, lacking seasonal dynamics. Although the LER index provides insights, its reliance on selected landscape metrics and their assigned weights means it may not capture all dimensions of ecological risk in riparian environments. Furthermore, the scale sensitivity of the results is influenced by the grid scale, requiring adjustments for finer-scale designs.

4.3. Policy Recommendations

Empirical findings underscore that the sustainable development of river shoreline spaces remains an urgent challenge, necessitating ecological spatial zoning to balance conservation with local economic enhancement. Based on our zoning framework, the following place-based governance recommendations are proposed:

High ESV–High LER Zone (Protection Priority Area): Despite possessing forests and water bodies with high economic value, natural and anthropogenic disturbances make them susceptible to conversion to other land uses. The key lies in establishing legally binding, differentiated riparian buffer zones. This entails immediately subjecting the core zones of such areas to stringent development and construction prohibitions in line with ecological protection red line mandates, irrespective of whether they are currently formally included within the red line. Following the directives of superior plans, it is essential to prioritize the execution of the Three-North Shelter Forest Project, enhance the "holistic management of mountains, rivers, forests, farmlands, lakes, grasslands, and sandy lands," and ensure the establishment of stream ecological buffers. Such targeted buffering is expected to stabilize and gradually reduce local LER by mitigating external disturbances, while simultaneously preserving the existing high ESV [60–64].

Low ESV–High LER Zone (Urgent Restoration Area): This area primarily consists of arable land, construction land, and idle land with low ecological function and economic value. Farming and industrial expansion in these regions have infringed on the riparian buffer zones, resulting in convergent landscapes and degraded habitats. Soil erosion is a particularly severe issue, primarily caused by insufficient vegetation cover and loose soil texture. For these sites, we recommend strictly enforcing cropland boundaries, restoring farmland to forests and grasslands in severely disturbed areas, and enhancing the management and protection of forests and grasslands. Targeted restoration at key

nodes should be conducted through soil improvement and the reconstruction of vegetation communities [65].

Low ESV–Low LER Zone (Built Environment Optimization Area): This area primarily comprises cultivated land, construction land, and grassland, located mainly within highly urbanized regions. Extensive human activities have introduced problems, including riverbank hardening, canalization, and plant homogenization. However, policy-driven ecological land use adjustments have established a relatively stable ecological structure. Management should focus on cost-effectively enhancing the provision of ecosystem services within the built environment, rather than targeting further reduction in LER. In addition, the potential of existing rivers, parks, and reservoirs should be harnessed to construct artificial wetlands, thereby enhancing the cleansing function of riparian buffers. Moreover, ecological riverbank restoration and retrofitting are crucial for maintaining slope stability and restoring the river's self-purification capacity. Successful implementation is expected to gradually increase urban ESV, while LER is likely to remain within its controlled low range.

High ESV–Low LER Zone (Strict Conservation Area): It is primarily composed of lands with significant ecological functions, particularly water bodies, wetlands, and grasslands. The ample water supply sustains flourishing riparian vegetation, which promotes a stable ecosystem structure and positive feedback cycles that favor the continuous generation of high ESV. The ecosystem remains healthy, as human activities have little effect on its structure and functioning. Consequently, management ought to prioritize natural preservation and appropriately limit the degree and range of human interference. Strategies such as partial fallowing and natural restoration are advised. Additionally, setting up a long-term ecological monitoring station within this zone will transform it into a scientific benchmark for evaluating restoration successes elsewhere and for refining regional ecological policies.

Incorporating this zoning strategy into the implementation rules of relevant policies is a crucial step toward realizing the strategic goals of ecological protection and high-quality development in the Yellow River Basin.

4.4. Limitations and Prospects

While this study yields meaningful findings, several limitations should be acknowledged. First, although the 30 m resolution land use data is suitable for regional-scale analysis, it may not adequately capture more nuanced ecological processes within riparian zones. Second, the ESV estimation relies primarily on static value equivalent factors, which cannot fully reflect the dynamics of ecosystem services across phenological stages or under varying ecosystem health conditions. Finally, the absence of structured scenario-based simulation analysis means the proposed measures require strengthening in terms of operability, quantification, and foresight. Future research could integrate higher-resolution remote sensing data to depict the ecological patterns of river shorelines at a finer scale. Simultaneously, introducing process models to conduct biophysical assessment and dynamic simulation of key services such as water conservation and soil retention would allow cross-validation with value-based assessment, thereby enhancing the objectivity of the analysis. This will elucidate the impact on the spatiotemporal coupling relationship between ESV and LER, thereby strengthening the decision-support capability of the research and serving the practical management needs of watershed ecological protection and high-quality development more effectively.

5. Conclusions

This study developed a comprehensive evaluation framework integrating ESV, LER, and I_{eb}. This framework was applied to systematically reveal the spatiotemporal evolution of ecological risk in the shoreline space of the Lan–Bai Metropolitan Area, located in the

upper Yellow River region, from 1990 to 2020. The study found that regional land use exhibits a trend of urban expansion encroaching upon ecological spaces, leading to an overall decline in ESV and a net loss of ecological capital. The decrease in LER, meanwhile, reflects a structural shift in the landscape pattern from dynamic disturbance toward a "low-functionality, low-disturbance" steady state. The core methodological contribution lies in the robust identification of the ESV and LER synergy. By introducing an Empirical Bayesian correction, the framework effectively mitigates interference from spatial heterogeneity. Furthermore, by employing natural process-oriented grids and riparian buffers for analysis, the study overcomes the limitations inherent to traditional administrative boundaries. This approach constructs an explicitly spatial zoning model tailored to sensitive river shoreline environments. This framework provides a basis for refined ecological management and regulation within the Yellow River Basin. It also offers a replicable analytical paradigm for integrated research in similar ecologically fragile regions globally. Future research could enhance the dynamic and predictive capabilities of such assessments by integrating high-resolution remote sensing data and process-based ecosystem models.

Supplementary Materials: The following supporting information can be downloaded at: https://www.mdpi.com/article/10.3390/land15020317/s1, Figure S1: Comparison of ESV across grid scales (250 m, 5000 m, and 1000 m) in the riparian zone of the LBMA, 2020. Figure S2. Comparison of LER across grid scales (250 m, 500 m, and 1000 m) in the riparian zone of the LBMA, 2020. Figure S3: Comparison of bivariate LISA-based ecological zoning results across grid scales (250 m, 500 m, and 1000 m), 2020.

Author Contributions: Conceptualization, Z.C. and J.Y.; methodology, Z.C. and J.Y.; software, J.Y. and M.H.; validation, J.Y., M.H. and H.W.; formal Analysis, J.Y.; investigation, J.Y., M.H. and H.W.; data curation, Y.S., M.H. and H.W.; writing—original draft preparation, J.Y. and M.H.; writing—review & editing, Z.C., J.Y. and H.W.; visualization, Z.C., J.Y. and M.H.; supervision, Z.C. and Y.S.; project administration, Z.C. and Y.S.; funding acquisition, Z.C. All authors have read and agreed to the published version of the manuscript.

Funding: This research was funded by the Lanzhou Jiaotong University-Tianjin University Joint Innovation Foundation of China (Grant NO. LH2024007), the Philosophy and Social Sciences Planning Project of Gansu Province (Grant NO. 2023YB033) and the Natural Science Foundation of Gansu Province (Grant NO. 25JRRA175).

Data Availability Statement: The original contributions presented in the study are included in the article; further inquiries can be directed to the corresponding author.

Conflicts of Interest: The authors declare no conflicts of interest.

References

1. Fu, S.; Zhang, J.; Li, Y.; Chen, W.; Zhang, Y.; Yi, K.; Dai, Y. Environmental variables affect the effectiveness of ecosystem services of ecological restoration project: Evidence from Xiangjiang River Basin-Dongting Lake. *J. Clean. Prod.* **2025**, *527*, 146739. [CrossRef]
2. Wang, C.; Chang, Y.; Guo, B.; Liu, P. Forecasting and Evaluation of Ecosystem Services Supply-Demand Under SSP-RCP Scenarios in the Henan Segment of the Yellow River Basin, China. *Remote Sens.* **2025**, *17*, 1067. [CrossRef]
3. Xu, C.; Tian, Z.; Lu, Y.; Yin, Z.; Du, Z. Analysis of the Spatiotemporal Variation Characteristics and Driving Forces of Crops in the Yellow River Basin from 2000 to 2023. *Remote Sens.* **2025**, *17*, 2934. [CrossRef]
4. Mou, X.; Zhang, X.; Wang, X.; Wang, J.; Rao, S.; Huang, J.; Chai, H. Ecological Change Assessment and Protection Strategy in the Yellow River Basin. *Strateg. Study Chin. Acad. Eng.* **2022**, *24*, 113–121. [CrossRef]
5. Shuangmi, X.; Wenzhu, Z.; Bin, W.; Shengquan, L.; Guanhai, G.; Yanhua, L. Evaluating the migration of boundary river shorelines and coastal land cover changes for the Beilun River between China and Vietnam. *J. Hydrol. Reg. Stud.* **2025**, *57*, 102167. [CrossRef]
6. Cole, L.J.; Stockan, J.; Helliwell, R. Managing riparian buffer strips to optimise ecosystem services: A review. *Agric. Ecosyst. Environ.* **2020**, *296*, 106891. [CrossRef]

7. Wang, X.; Zhou, L.; Song, Y.; Wang, S.; Chen, H.; Gao, H.; Sun, Q.; Guo, Z.; Wei, W.; Lyu, R.; et al. Dramatic 2d/ 3d Differences in Urban Grey-Green Space Configurations Proportion and the Nonlinear Effects of the Thermal Environment. 2025. Available online: https://ssrn.com/abstract=5216323 (accessed on 2 January 2026).
8. Ma, L.; Li, S.; Zhang, W.; Li, J. Identification of Spatial Fairness and Obstacle Factor of Public Service Facilities from Multigradient Perspective: Lan-Bai Urban Agglomeration. *J. Urban Plan. Dev.* **2025**, *151*, 05025017. [CrossRef]
9. Zhao, X.; Li, J.; Ruan, F.; Zou, Z.; He, X.; Zhou, C. Spatiotemporal Dynamics and Multi-Scenario Projections of the Land Use and Habitat Quality in the Yellow River Basin: A GeoDetector-PLUS-InVEST Integrated Framework for a Coupled Human–Natural System Analysis. *Remote Sens.* **2025**, *17*, 2181. [CrossRef]
10. Costanza, R.; d'Arge, R.; de Groot, R.; Farber, S.; Grasso, M.; Hannon, B.; Limburg, K.; Naeem, S.; O'Neill, R.V.; Paruelo, J.; et al. The value of the world's ecosystem services and natural capital. *Nature* **1997**, *387*, 253–260. [CrossRef]
11. Costanza, R.; de Groot, R.; Braat, L.; Kubiszewski, I.; Fioramonti, L.; Sutton, P.; Farber, S.; Grasso, M. Twenty years of ecosystem services: How far have we come and how far do we still need to go? *Ecosyst. Serv.* **2017**, *28*, 1–16. [CrossRef]
12. Gao, L.; Tao, F.; Liu, R.; Wang, Z.; Leng, H.; Zhou, T. Multi-scenario simulation and ecological risk analysis of land use based on the PLUS model: A case study of Nanjing. *Sustain. Cities Soc.* **2022**, *85*, 104055. [CrossRef]
13. Rezvani, A.; Cavalli, M.; Crema, S.; Djodjic, F.; Futter, M.; Ferreira, C.S.S.; Haozhi, P.; Kalantari, Z. A holistic framework for wetland placement and ecosystem service delivery by integrating landscape connectivity and participatory decision analysis in two Swedish catchments. *J. Hydrol. Reg. Stud.* **2025**, *61*, 102669. [CrossRef]
14. Xu, W.; Wang, J.; Zhang, M.; Li, S. Construction of landscape ecological network based on landscape ecological risk assessment in a large-scale opencast coal mine area. *J. Clean. Prod.* **2021**, *286*, 125523. [CrossRef]
15. Xie, G.D.; Zhang, C.X.; Zhang, L.M.; Chen, W.H.; Li, S.M. Improvement of the Evaluation Method for Ecosystem Service Value Based on Per Unit Area. *J. Nat. Resour.* **2015**, *30*, 1243–1254. [CrossRef]
16. Gu, F.; Xu, G.; Wang, B.; Cheng, Y.; Xu, M.; Li, J. Spatiotemporal variation and drivers of ecosystem service value: A case study in Ziwuling area, Loess plateau. *J. Environ. Manag.* **2025**, *393*, 127053. [CrossRef]
17. Yang, Q.; Liu, G.; Giannetti, B.F.; Agostinho, F.; Almeida, C.M.; Casazza, M. Emergy-based ecosystem services valuation and classification management applied to China's grasslands. *Ecosyst. Serv.* **2020**, *42*, 101073. [CrossRef]
18. Athukorala, D.; Murayama, Y.; Bandara, C.M.M.; Lokupitiya, E.; Hewawasam, T.; Gunatilake, J.; Karunaratne, S. Effects of urban land change on ecosystem service values in the Bolgoda Wetland, Sri Lanka. *Sustain. Cities Soc.* **2024**, *101*, 105050. [CrossRef]
19. Zhang, Y.; Wang, Y. How does urbanization evolve heterogeneously in urbanized, urbanizing, and rural areas of China? Insights from ecosystem service value. *Geogr. Sustain.* **2025**, *6*, 100254. [CrossRef]
20. Basu, T.; Das, A.; Das, K.; Pereira, P. Urban expansion induced loss of natural vegetation cover and ecosystem service values: A scenario-based study in the siliguri municipal corporation (Gateway of North-East India). *Land Use Policy* **2023**, *132*, 106838. [CrossRef]
21. Yang, S.; Jin, Z. Impact of road network expansion on landscape ecological risk and soil erosion sensitivity on the Luochuan Tableland of the Chinese Loess Plateau. *Reg. Environ. Change* **2024**, *24*, 37. [CrossRef]
22. Wang, N.; Yan, J.; Su, F. Landscape pattern changes and ecological risk assessment of major bays in the Philippines. *Ocean Coast. Manag.* **2024**, *251*, 107085. [CrossRef]
23. Jiang, Y.; Zhou, L.; Wang, B.; Zhang, Q.; Gao, H.; Wang, S.; Cui, M. The impact of gradient expansion of urban–rural construction land on landscape fragmentation in typical mountain cities, China. *Int. J. Digit. Earth* **2024**, *17*, 2310093. [CrossRef]
24. Gao, B.; Wu, Y.; Li, C.; Zheng, K.; Wu, Y.; Wang, M.; Fan, X.; Ou, S. Multi-Scenario Prediction of Landscape Ecological Risk in the Sichuan-Yunnan Ecological Barrier Based on Terrain Gradients. *Land* **2022**, *11*, 2079. [CrossRef]
25. Gabisa, M.; Tiye, F.S.; Mammo, S. Impacts of land use land cover changes on wetland ecosystem services in Dandi Lake, Oromia, Ethiopia: An analysis using Google Earth Engine and machine learning. *J. Nat. Conserv.* **2026**, *89*, 127146. [CrossRef]
26. Li, Y.; Liu, J.; Zhu, Y.; Wu, C. Assessment of Landscape Ecological Risks Driven by Land Use Change Using Multi-Scenario Simulation: A Case Study of Harbin, China. *Land* **2025**, *14*, 947. [CrossRef]
27. Feng, B.; Zhou, J.; Hu, L.; Liu, Z.; Yang, Y.; Yang, S.; Ni, J.; Bai, W.; Zhao, S. Land Use and Ecosystem Service Value Spatiotemporal Dynamics, Topographic Gradient Effect and Their Driving Factors in Typical Alpine Ecosystems of the East Qinghai-Tibet Plateau: Implications for Conservation and Development. *Ecol. Evol.* **2025**, *15*, e71125. [CrossRef]
28. Li, J.; Hu, D.; Wang, Y.; Chu, J.; Yin, H.; Ma, M. Study of identification and simulation of ecological zoning through integration of landscape ecological risk and ecosystem service value. *Sustain. Cities Soc.* **2024**, *107*, 105442. [CrossRef]
29. Bian, J.; Chen, W.; Zeng, J. Ecosystem services, landscape pattern, and landscape ecological risk zoning in China. *Environ. Sci. Pollut. Res.* **2023**, *30*, 17709–17722. [CrossRef]
30. Chen, D.; Guo, K.-R.; Zeng, W.; Wang, F.-H. Zoning-grading optimization of watershed ecological security network integrating function and structure: A case study in the Three Gorges Reservoir Area. *J. Clean. Prod.* **2026**, *538*, 147160. [CrossRef]

31. Ma, L.; Li, J.; Wang, X.; Zhang, W.; Tao, T.; Zhong, Y. Evolution and simulation optimization of rural settlements in urban-rural integration areas from a multi-gradient perspective: A case study of the Lan-Bai urban agglomeration in China. *Habitat Int.* **2024**, *153*, 103203. [CrossRef]
32. Liang, Z.; Yuefeng, J.; Chenghu, Z.; Zhifeng, L.I.U.; Qinke, S.U.N. Spatial characteristics and driving factors of gradient expansion of mountainous towns in China. *Acta Geogr. Sin.* **2025**, *80*, 2692–2707. [CrossRef]
33. Wang, Y.; Ge, J.; Zhang, Y.; Lu, J.; Zhang, Y.; Ma, F. Health assessment of the current situation of rivers and discussion on ecological restoration strategies: A case study of the Gansu province section of the Bailong river. *Ecol. Indic.* **2024**, *163*, 112038. [CrossRef]
34. Wang, Z.; Shi, P.; Shi, J.; Zhang, X.; Liu, Y. Research on the relationship between urban space and ecological environment evolution at the grid scale: A case study of Lanzhou City. *Cities* **2025**, *163*, 106006. [CrossRef]
35. Wang, L.; Liu, X.; Lei, J.; Ma, J.; Zhang, L.; Liu, X. How the land use change impact on ecological vulnerability in the Lanzhou-Baiyin section of the Yellow River Basin, China. *Environ. Sustain. Indic.* **2025**, *27*, 100779. [CrossRef]
36. Xie, Y.; Zhu, Q.; Bai, H.; He, H.; Zhang, Y. Combining ecosystem service value and landscape ecological risk to subdivide the riparian buffer zone of the Weihe River in Shaanxi. *Ecol. Indic.* **2024**, *166*, 112424. [CrossRef]
37. Luan, C.; Liu, R.; Li, Y.; Zhang, Q. Comparison of various models for multi-scenario simulation of land use/land cover to predict ecosystem service value: A case study of Harbin-Changchun Urban Agglomeration, China. *J. Clean. Prod.* **2024**, *478*, 144012. [CrossRef]
38. Das, M.; Das, A. Dynamics of Urbanization and its impact on Urban Ecosystem Services (UESs): A study of a medium size town of West Bengal, Eastern India. *J. Urban Manag.* **2019**, *8*, 420–434. [CrossRef]
39. Sui, L.; Yan, Z.; Li, K.; Wang, C.; Shi, Y.; Du, Y. Prediction of ecological security network in Northeast China based on landscape ecological risk. *Ecol. Indic.* **2024**, *160*, 111783. [CrossRef]
40. Xue-Bin, Z.; Pei-Ji, S.; Jun, L.; Hai-Long, L.; Wei, W. The Ecological Risk Assessment of Arid Inland River Basin at the Landscape Scale:A Case Study on Shiyang River Basin. *J. Nat. Resour.* **2014**, *29*, 410–419.
41. Wang, W.; Chen, Y.; Du, Z.; Bi, S.; Zhang, Q.; Ye, T. Ecological restoration zoning and its driving factors in Beijing-Tianjin-Hebei based on landscape ecological risk and ecosystem services. *Ecol. Indic.* **2025**, *178*, 114086. [CrossRef]
42. Assunção, R.M.; Reis, E.A. A new proposal to adjust Moran's I for population density. *Stat. Med.* **1999**, *18*, 2147–2162. [CrossRef]
43. Lee, S.-I. Developing a bivariate spatial association measure: An integration of Pearson's r and Moran's I. *J. Geogr. Syst.* **2001**, *3*, 369–385. [CrossRef]
44. Marshall, R.J. Mapping Disease and Mortality Rates Using Empirical Bayes Estimators. *J. R. Stat. Society. Ser. C Appl. Stat.* **1991**, *40*, 283–294. [CrossRef]
45. Mwasenga, J.M.; Mjemah, I.C. Socio-Economic Feasibility for Implementation of Environmental Legislation along the Riparian Buffer Zones in Urban Rivers of Northern Tanzania. *Urban Sci.* **2023**, *7*, 73. [CrossRef]
46. Wang, J.; He, T.; Lin, Y. Changes in ecological, agricultural, and urban land space in 1984–2012 in China: Land policies and regional social-economical drivers. *Habitat Int.* **2018**, *71*, 1–13. [CrossRef]
47. Sun, S.; Chu, X.; Dong, W.; Wei, C.; Li, Z.; Song, S.; He, T. Research on the interaction of "tourism development-land use-landscape pattern" since the 1990s in a small karst basin, China. *Environ. Sci. Pollut. Res.* **2023**, *30*, 46869–46883. [CrossRef]
48. Gong, J.; Cao, E.; Xie, Y.; Xu, C.; Li, H.; Yan, L. Integrating ecosystem services and landscape ecological risk into adaptive management: Insights from a western mountain-basin area, China. *J. Environ. Manag.* **2021**, *281*, 111817. [CrossRef]
49. Ye, Y.; Zhang, J.; Wang, T.; Bai, H.; Wang, X.; Zhao, W. Changes in Land-Use and Ecosystem Service Value in Guangdong Province, Southern China, from 1990 to 2018. *Land* **2021**, *10*, 426. [CrossRef]
50. Kong, W.; Shen, W.; Yu, C.; Niu, L.; Zhou, H.; Zhang, Z.; Guo, S. The neglected cost: Ecosystem services loss due to urban expansion in China from a triple-coupling perspective. *Environ. Impact Assess. Rev.* **2025**, *112*, 107827. [CrossRef]
51. Rahman, H.; Muhammad, H.; Indrayani, P.; Triyatno, T. Spatial Assessment of Landscape Structure Changes and Ecological Connectivity in Pariaman. *J. Remote Sens. GIS Technol.* **2020**, *6*, 10–22. [CrossRef]
52. Meng, F.; Dong, L.; Zhang, Y. Spatiotemporal Dynamic Analysis and Simulation Prediction of Land Use and Landscape Patterns from the Perspective of Sustainable Development in Tourist Cities. *Sustainability* **2023**, *15*, 14450. [CrossRef]
53. Yang, J.; Xie, B.; Zhang, D. Spatial–temporal evolution of ESV and its response to land use change in the Yellow River Basin, China. *Sci. Rep.* **2022**, *12*, 13103. [CrossRef] [PubMed]
54. Ma, M.; He, Y.; Sun, Y.; Cui, H.; Zang, H. Land Use Modeling and Predicted Ecosystem Service Value Under Different Development Scenarios: A Case Study of the Upper–Middle Yellow River Basin, China. *Land* **2025**, *14*, 115. [CrossRef]
55. Shi, S.; Yan, T.; Zhao, W.; Qin, W.; Bai, Z. Longitudinal dynamic characteristics of ecosystem services and its response to natural and anthropogenic interactions in ecologically fragile areas. *J. Environ. Manag.* **2025**, *394*, 127253. [CrossRef]
56. Xiong, Y.; Li, Y.; Yang, Y. Landscape Ecological Risk Assessment of Peri-Urban Villages in the Yangtze River Delta Based on Ecosystem Service Values. *Sustainability* **2025**, *17*, 7014. [CrossRef]
57. Wu, C.; Guo, X.; Liu, F.; Dai, E. Land use zoning planning based on ecosystem services can improve regional comprehensive benefits. *Ecol. Indic.* **2025**, *181*, 114420. [CrossRef]

58. Nie, X.Y.; Wang, C.; Li, K.M.; Gao, F.Y.; Huang, W.-Z.; Li, X. Spatiotemporal analysis of landscape ecological risk and its influencing factors based on land cover changes in the Hexi Corridor, Northwest China, 2000–2020. *Environ. Sustain. Indic.* **2025**, *28*, 100888. [CrossRef]
59. Lin, Y.; Zhang, F.; Jin, Y.; Wen, L.; Yu, Y.; Zhang, L.; Weng, A.; Ge, Y. Spatial non-stationarity effects of the driving factors on landscape ecological risk: A case of the Xiamen-Zhangzhou-Quanzhou Urban Agglomeration, China. *Ecol. Indic.* **2024**, *167*, 112660. [CrossRef]
60. Brumberg, H.; Beirne, C.; Broadbent, E.N.; Almeyda Zambrano, A.M.; Almeyda Zambrano, S.L.; Quispe Gil, C.A.; Lopez Gutierrez, B.; Eplee, R.; Whitworth, A. Riparian buffer length is more influential than width on river water quality: A case study in southern Costa Rica. *J. Environ. Manag.* **2021**, *286*, 112132. [CrossRef]
61. Luke, S.H.; Slade, E.M.; Gray, C.L.; Annammala, K.V.; Drewer, J.; Williamson, J.; Agama, A.L.; Ationg, M.; Mitchell, S.L.; Vairappan, C.S.; et al. Riparian buffers in tropical agriculture: Scientific support, effectiveness and directions for policy. *J. Appl. Ecol.* **2019**, *56*, 85–92. [CrossRef]
62. Lind, L.; Hasselquist, E.M.; Laudon, H. Towards ecologically functional riparian zones: A meta-analysis to develop guidelines for protecting ecosystem functions and biodiversity in agricultural landscapes. *J. Environ. Manag.* **2019**, *249*, 109391. [CrossRef] [PubMed]
63. Paarlberg, A.; Sena, G.; Loc, H.H.; Schultner, J. Understanding Stakeholder Perspectives on the Implementation and Management of Riparian Buffer Zones in the Santa Lucía River Basin, Uruguay. *Environ. Manag.* **2025**, *75*, 2596–2613. [CrossRef] [PubMed]
64. Jiang, P.; Cheng, L.; Li, M.; Zhao, R.; Duan, Y. Impacts of LUCC on soil properties in the riparian zones of desert oasis with remote sensing data: A case study of the middle Heihe River basin, China. *Sci. Total Environ.* **2015**, *506–507*, 259–271. [CrossRef] [PubMed]
65. Butt, A.N.; Rigoni, C. The Green Blueprint: Designing Future Cities with Urban Green Infrastructure and Ecosystem Services in the UK. *Land* **2025**, *14*, 1306. [CrossRef]

Disclaimer/Publisher's Note: The statements, opinions and data contained in all publications are solely those of the individual author(s) and contributor(s) and not of MDPI and/or the editor(s). MDPI and/or the editor(s) disclaim responsibility for any injury to people or property resulting from any ideas, methods, instructions or products referred to in the content.